Accepted Manuscript

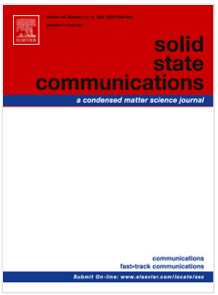

Polarization memory in single Quantum Dots

E. Poem, S. Khatsevich, Y. Benny, I. Marderfeld, A. Badolato, P.M. Petroff, D. Gershoni

PII: S0038-1098(09)00255-5
DOI: 10.1016/j.ssc.2009.04.046
Reference: SSC 10090

To appear in: *Solid State Communications*

Received date: 9 February 2009
Accepted date: 27 April 2009

Please cite this article as: E. Poem, S. Khatsevich, Y. Benny, I. Marderfeld, A. Badolato, P.M. Petroff, D. Gershoni, Polarization memory in single Quantum Dots, *Solid State Communications* (2009), doi:10.1016/j.ssc.2009.04.046

Polarization memory in single Quantum Dots

E. Poem*[,a], S. Khatsevich[a], Y. Benny[a], I. Marderfeld[a], A. Badolato[b], P. M. Petroff[b], D. Gershoni[a]

[a] *Department of physics, The Technion - Israel institute of technology, Haifa, 32000, Israel*
[b] *Materials Department, University of California Santa Barbara, CA, 93106, USA*

Abstract

We measured the polarization memory of excitonic and biexcitonic optical transitions from single quantum dots at either positive, negative or neutral charge states. Positive, negative and no circular or linear polarization memory was observed for various spectral lines, under the same quasi-resonant excitation below the wetting layer band-gap. We developed a model which explains both qualitatively and quantitatively the experimentally measured polarization spectrum for all these optical transitions. We consider quite generally the loss of spin orientation of the photogenerated electron-hole pair during their relaxation towards the many-carrier ground states. Our analysis unambiguously demonstrates that while electrons maintain their initial spin polarization to a large degree, holes completely dephase.

Key words: A. Semiconductors, D. Quantum Dots, D. Polarization Memory
PACS: 78.67.Hc, 73.21.La, 42.25.Ja

1. Introduction

Charge-carriers in semiconductor quantum dots (QDs) are three-dimensionally confined and quite isolated from their immediate environment. Therefore, their spin states are relatively protected, resulting in long lifetimes and slow dephasing rates [1]. As such, they are considered by many as candidates for stationary, solid-state qubits [2, 3, 4], the building blocks for quantum information processing [5].

The spin states of charge carriers in semiconductors can be addressed externally by means of optical orientation [6]. This possibility establishes, in principle, external avenues for 'reading', 'writing' and manipulating these in-matter, stationary qubits [7, 8, 9, 10, 11, 12]. Many recent efforts have been therefore devoted to study the optical properties of semiconductor quantum dots in general [13, 14], and their polarization sensitive spectroscopy in particular [15, 16, 17, 18, 19]. Correlations between the polarization of the light which excites QDs resonantly [11, 20] or quasi-resonantly [1, 7] and the polarization of the photoluminescence (PL) that they consequently emit have been studied both in single [7, 16, 21, 22, 23] and in ensembles of QDs [20, 24, 25, 26, 27]. In particular, effects of positive and negative [28, 27, 29, 30] circular and linear [15, 20, 22] polarization memory have been experimentally observed and theoretically discussed [28, 29]. Most of these studies, however, presented one particular experimental observation, pertaining to a given charge state, or particular excitation conditions. Thus, the gained understanding have not been either compared with, or applied to a wider range of observations.

In this work, we describe comprehensive experimental and theoretical study of the degree of circular and linear polarization memory (DCPM and DLPM, respectively) in quasi-resonantly excited single QDs. We were able to identify and investigate excitonic and biexcitonic transitions from seven different positive, negative and neutral charge states of the same QD. The experimentally observed quite rich polarization memory spectra reveal positively charged spectral lines with positive DCPM, negatively charged lines with either positive or negative DCPM and some lines which have no polarization memory at all. In, addition, we find that none of the spectral lines at this, quasi-resonant excitation conditions, closely below the

*Corresponding author
Email address: poem@technion.ac.il (E. Poem)

wetting layer bandgap energy, exhibit DLPM.

Our experimental observations are analyzed using a many-carrier, full configuration interaction (FCI) model [19]. We use the model, which takes into account also the electron-hole exchange interaction, for calculating the confined many carriers collective states and optical transitions between them [19].

The polarization memory effect is introduced into the model by allowing only the quasi resonantly excited spin polarized electron hole pair to lose its spin orientation during its relaxation to the ground many carrier states. The reasoning behind this assumption is the vast body of experimental and theoretical evidences that QD confined ground state charge carriers do not lose their spin orientation within a typical radiative time scale (1 nanosecond) [1, 21, 31, 32].

The relaxation to the ground state is followed by radiative recombination which we straightforwardly calculate by our FCI model [19].

Comparison between the experimental observations and the theoretical model yields quantitative agreement with all the obseved spectral lines. This agreement unambiguously demonstrate that while electrons memorize their initial spin polarization during their thermalization, holes completely dephase.

2. Experimental methods

2.1. Sample

The studied sample was grown by molecular beam epitaxy on a (001) oriented GaAs substrate. One layer of strain-induced InGaAs QDs was deposited in the center of a 285 nm thick intrinsic GaAs layer. The GaAs layer was placed between two distributed Bragg reflecting mirrors (DBRs), made of 25 (bottom DBR) and 10 (top DBR) periods of pairs of AlAs/GaAs quarter wavelength thick layers. This constitutes a one optical wavelength in matter microcavity for light emitted due to recombination of QD confined e-h pairs in their respective lowest energy states.

In order to apply electric fields on the QDs and thereby change their charge state, a p-i-n structure was formed by n- (p-) doping the bottom (top) DBR, while leaving the GaAs spacer intrinsic. In addition, a 10 nm thick AlAs barrier was grown inside the GaAs spacer between the p-type region and the QDs. This barrier prolongs the hole's tunneling time into (out of) the QDs at forward (reverse) bias, with respect to the tunneling time of the electron. In this way the QDs could have been charged negatively or positively upon forward or reverse bias, respectively.

2.2. Optical characterization

For the optical measurements the sample was mounted on the cold finger of a He-flow cryostat, maintaining temperature of about 20K. A X60 insitu microscope objective was used in order to both focus the exciting beam on the sample surface and collect the emitted light. The collected light was dispersed by a 1 meter monochromator and detected by an electrically-cooled CCD array detector with spectral resolution of about 10 μeV per one CCD camera pixel. The polarization of the exciting beam was defined and that of the emitted light was analyzed by using two sets of two computer controlled liquid crystal variable retarders and a linear polarizer.

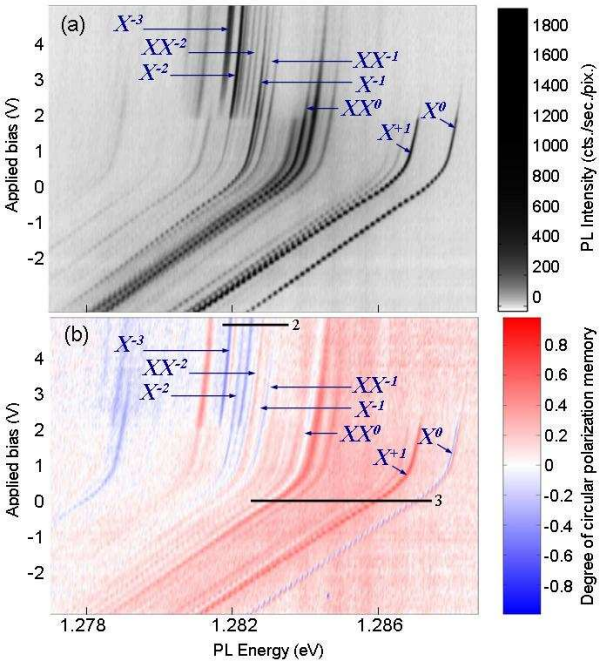

Figure 1: (Color online) Bias dependent PL spectra (a) and DCPM (b) from a single QD excited at 1.369 eV. The black horizontal lines marked 2 and 3 indicate the bias and spectral ranges from which Figs. 2 and 3 were obtained.

In Fig. 1(a) we present bias dependent photoluminescence (PL) spectra from one single QD, optically excited at 1.369 eV. At this energy, a few meV below the bandgap of the InAs wetting layer, the

QDs are quasi-resonantly excited [16]. At reverse bias the spectral lines are red-shifted due to the applied electric field, and lines due to optical transitions in the presence of positive charges are enhanced. At forward bias, flat-band conditions are reached and spectral lines due to the presence of negative charges appear. The various spectral lines are identified by their bias dependence, their order of appearance, and by their polarized fine structures [19]. In Fig. 1(b) we present the DCPM spectra as a function of the bias. The DCPM is defined as $P_{circ} = (I_+^+ - I_-^+)/(I_+^+ + I_-^+)$, where I stands for the PL intensity, and the superscript (subscript) $+$ $(-)$ stands for right- (left-) hand circular polarization of the exciting (emitted) light. Clearly, the DCPM of each and every spectral line is almost bias independent. While for all positive lines the DCPM is positive, different negative lines have different DCPM signs.

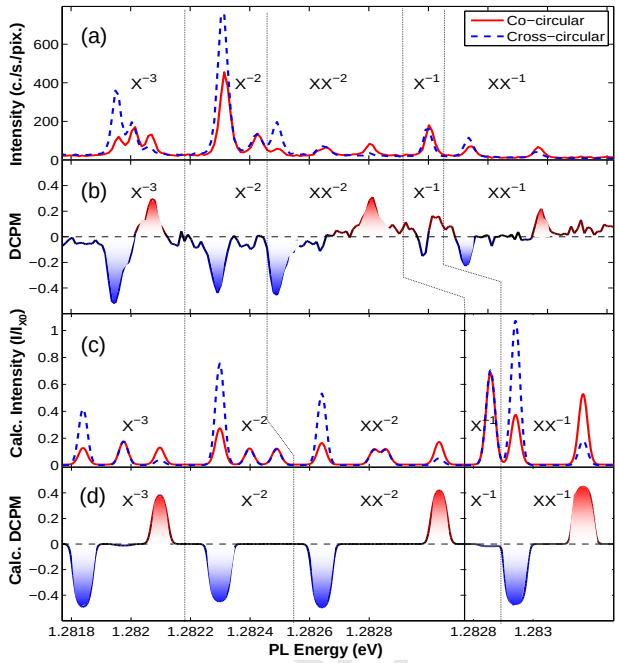

Figure 2: (Color online) (a) measured and (c) calculated polarization sensitive spectra at 4.9 V. The solid red (dashed blue) line represents spectrum obtained with co- (cross-) circularly polarized excitation and detection: $I_{co} = I_+^+$ $(I_{cross} = I_-^+)$. (b) measured and (d) calculated degree of circular polarization memory. The dotted vertical lines are guides to the eye.

In Fig. 2(a) we present spectra obtained at a forward bias of 4.9 V. At this voltage the QD is negatively charged with 1 - 3 electrons. The solid red (dashed blue) line represents the spectrum obtained when the excitation and collection are co- (cross-) circularly polarized. In Fig. 2(b) we present the corresponding DCPM. In Fig. 2 one clearly observes again that the DCPM sign depends on the specific optical transition. Some spectral lines show positive memory, like all the lines associated with positive charge do. Some show no polarization memory, and some show negative polarization memory.

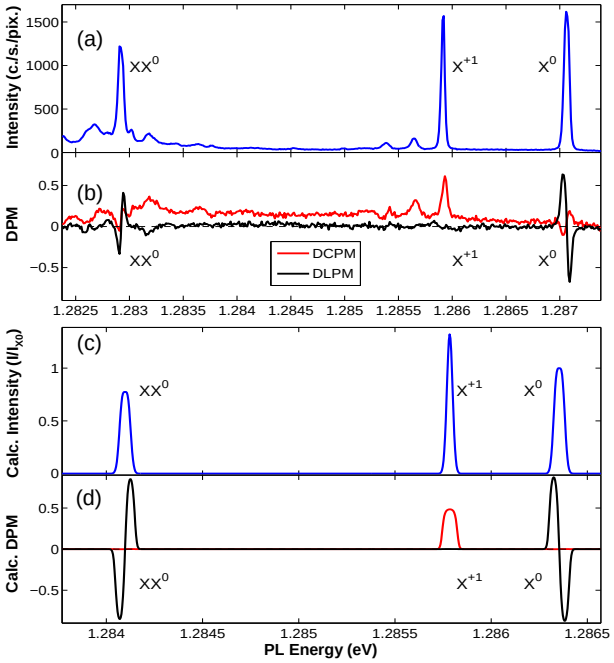

Figure 3: (Color online) (a) measured and (c) calculated unpolarized PL spectra at 0 V. (b) measured and (d) calculated degrees of circular (red line) and linear (black line) polarization memory.

In Fig. 3(a) we present the spectrum obtained at 0 V. In Fig. 3(c) we present the measured DCPM and DLPM. The DLPM is defined as $P_{lin} = (I_H^H - I_V^H)/(I_H^H + I_V^H)$, where the horizontal (H) [vertical (V)] direction is determined by the polarization direction of the lower (higher) energy fine-structure component of the neutral exciton (X^0) line. The X^0 line shows no DCPM, and in total no DLPM either, since its H and V polarized fine-structure components are equally visible upon H linearly polarized excitation. We note that the X^{+1} (positively charged exciton) shows strong positive DCPM but no DLPM.

3. Theoretical Model

In order to explain these observations and to gain further insight into the phenomenon of polarization memory in optically excited single semiconductor quantum dots we developed a single-band, full configuration-interaction model, which includes the electron-hole exchange interaction (EHEI) [19]. We use the model to calculate the quantum dot's confined many-carrier states and the selection rules for optical transitions between these states. Prior to the optical excitation the states within 1 meV from the ground state of a given number of N_h holes and N_e electrons were considered to be populated with equal probability. This assumption is compatible with thermal distribution at the ambient temperature of the experiment. We consider the polarized quasi-resonant excitation at a given polarization by adding an additional electron-hole pair to these states. The spin state of the additional carriers are defined by their initial spin polarization, S_{exc}, dictated by the polarization of the exciting light, and by their spin dephasing during thermalization.

Quite generally, we describe the spin orientation loss by 4 probabilities which apply to each carrier independently. The probabilities $p_j^{e(h)}$ are for either spin orientation preservation, $j = 0$, or for spin rotations by π radians about the spatial directions x, y, and z for $j = 1, 2$ and 3, respectively. The spin states of the thermalized pair can now be represented by a 4x4 density matrix in the Hilbert space of the pair's spin states $\uparrow\Uparrow, \uparrow\Downarrow, \downarrow\Uparrow, \downarrow\Downarrow$:

$$\rho^{th} = \sum_{j,j'=0}^{3} p_j^e p_{j'}^h \sigma_j^e \otimes \sigma_{j'}^h |S_{exc}\rangle\langle S_{exc}| \sigma_j^{e\dagger} \otimes \sigma_{j'}^{h\dagger} \quad (1)$$

where $\sigma_j^{e(h)}$ are the Pauli matrices acting on the sub-space of electron ($\uparrow$) (hole ($\Uparrow$)) spin states and σ_0 is the unit matrix.

If one further assumes that the spin orientation loss (or dephasing) for both carrier types is isotropic, the number of independent probabilities to be considered is reduced to two. Thus: $p_1^{e(h)} = p_2^{e(h)} = p_3^{e(h)} = p^{e(h)}$ and $p_0^{e(h)} = 1 - 3p^{e(h)}$. We note here that defining these probabilities in the more frequently used terms of T_1 and T_2 times [1] is straightforward, if the thermalization times are known.

The additional pair increases the number of charge carriers to $N_h + 1$ holes and $N_e + 1$ electrons. The new many carrier states are restricted to these many carrier states which accommodate the photogenerated carriers with their spin orientation. For an initial state $|A\rangle$ of N_e electrons and N_h holes, the resulting density matrix which defines the states with the additional thermalized pair is given by

$$\rho_A = \sum_{\alpha,\beta} \rho_{\alpha\beta}^{th} \hat{x}_\alpha^\dagger |A\rangle\langle A| \hat{x}_\beta \quad (2)$$

where $\hat{x}_\alpha^\dagger$ is the creation operator of an electron-hole pair with spin α in any combination single elctron and single hole spatial states:

$$\hat{x}_\alpha^\dagger = \sum_{m,n} \hat{a}_{m,\alpha_e}^\dagger \hat{b}_{n,\alpha_h}^\dagger \quad (3)$$

where $\hat{a}_{m,\alpha_e}^\dagger$ ($\hat{b}_{n,\alpha_h}^\dagger$) is the creation operator of an electron (a hole) in the single electron (hole) spatial state m (n), and the spin state α_e (α_h), where the spin state of the electron-hole pair is $\alpha \equiv \{\alpha_e, \alpha_h\}$.

With this description of the N_e+1, N_h+1 state, we proceed by projecting it on all energy 'ground' states $|G\rangle$ within 1 meV of the lowest energy level of this number of charge carriers, which are the states which contribute to photoluminescence. We then conclude by calculating the energies ε and intensities for polarized optical transitions $I_{S_{em}}^G(\varepsilon)$ with polarization S_{em} from the ground state $|G\rangle$ to states of N_h holes and N_e electrons [19, 33]. The S_{em} polarized spectrum for S_{exc} polarized quasi-resonant excitation is then obtained by summing over all the thermally populated initial states $|A\rangle$ and over all optically excited $|G\rangle$ states contributing to the photoluminescence:

$$I_{S_{em}}^{S_{exc}}(\varepsilon) = \sum_{G,A} Tr(\rho_A |G\rangle\langle G|) \cdot I_{S_{em}}^G(\varepsilon) \quad (4)$$

where ρ_A is obtained from $|S_{exc}\rangle$ by Eq. 1 and Eq. 2.

The two probabilities p^e and p^h of Eq. 1 can now be found by comparing the measured DCPM and DLPM to the calculated ones. The values $p^e = 1/8$ and $p^h = 1/4$ describe very well the observations for this particular quasi-resonant excitation. These values mean that while the hole totally loses its polarization during the thermalization, the electron's degree of polarization is reduced to half. Kalevich *et al* [29] previously assumed a similar situation to successfully explain their observation of negative circular polarization memory in an ensemble of doubly-negatively charged QDs.

The calculated spectra for co- and cross- circularly polarized emission from a negatively charged

quantum dot with 1 up to 3 charges were added together to form the calculated polarization sensitive spectra in Fig. 2(c). Both single exciton and biexciton emissions were included. Gaussian broadening of 35 μeV was assigned for each allowed optical transition. The obtained calculated DCPM spectrum is presented in Fig. 2(d). By comparing the measured and calculated polarization sensitive spectra and DCPM, one clearly notes that all the features of the measured DCPM are given by this simple model. In Fig. 3(c) we present the calculated spectrum for the neutral exciton (X^0), the neutral biexciton (XX^0), and the singly positively charged exciton (X^{+1}). In Fig. 3(d) we present the corresponding calculated DCPM (red) and DLPM (black). The H (V) directions are along the long (short) semi-axes of the model QD [19]. The positive DCPM of the X^{+1} spectral line and the lack of DCPM from the neutral excitonic transitions are clearly reproduced by our model. In addition the model clearly reproduces the experimentally measured lack of DLPM from all the observed spectral lines at this quasi resonant excitation energy. We note here, however, that DLPM is observed in some cases of resonant excitations [15, 20, 22]. In these cases, (to be presented and discussed elsewhere), both carrier types do not completely lose their initial spin polarization orientation during the thermalization prior to the recombination.

We identify the main cause of the observed DCPM phenomena as the isotropic-EHEI induced energetic separation between states where the electron and hole spins are parallel, and those where they are anti-parallel. Since circularly polarized excitation always involve electron-hole pairs with anti-parallel spins, states with (anti-) parallel spins can be reached only in cases where one (none) of the carriers flips its spin, yielding negative (positive) circular polarization memory. We note that in the case of the doubly negatively charged exciton (X^{-2}), the appearance of negative DCPM for the lower-in-energy doublet indicates that the energy splitting between the two components of this doublet is smaller than the radiative width of the lines [29, 34]. Consequently, we set this particular EHEI energy to zero in our model [19].

As an illustration of the processes involved in the polarization memory, we schematically describe in Fig. 4 the case of quasi resonant excitation of the X^{-3} spectral line.

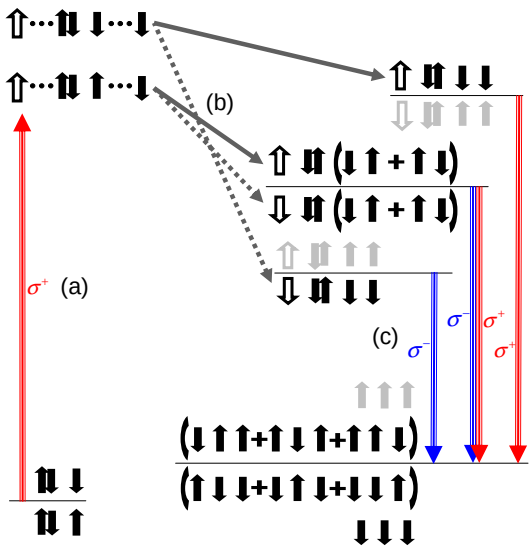

Figure 4: (Color online) Schematic description of the processes which lead to the observed DCPM among the X^{-3} spectral lines. The symbol $\Uparrow$ ($\downarrow$) represents a spin-up (down) hole (electron). the symbols are ordered from left to right in increasing energy order ($\boldsymbol{s}$, $\boldsymbol{p_x}$, $\boldsymbol{p_y}$). Gray color represent states which do not participate in the described process. (a) An electron-hole pair is photogenerated by a quasi-resonant $\boldsymbol{\sigma^+}$ polarized excitation and added to three QD electrons residing in their ground states. (b) During the thermalization, the hole spin projection along the growth direction is either preserved (solid dark-gray arrows), or flipped (dotted dark-gray arrows). The lowest (highest) energy levels of the ground $\boldsymbol{N_e = 4}$, $\boldsymbol{N_h = 1}$ states, is reached only if the hole flips (preserves) its spin orientation. The intermediate level is reached in both cases. (c) All three levels return via radiative recombination of an $\boldsymbol{s}$ shell electron hole pair to the same four-fold degenerate $\boldsymbol{N_e = 3}$, $\boldsymbol{N_h = 0}$ level, giving rise to spectral lines with positive, negative and no DCPM, respectively.

4. Summary

In summary, we measured positive, zero and negative degree of circular polarization memory in optical transitions from various negatively charged states of single quantum dots at quasi-resonant optical excitation. At the same conditions, transition originated from oddly positively charged states show only positive degree of circular polarization. All the observed spectral lines do not show appreciable degree of linear polarization memory. We developed a model which provides means for calculating polarization memory for any polarization state of the exciting light and any many carrier state of a single quantum dot. By applying the model to the case under study we provide quantitative agreement

with all the experimental observations. The agreement is achieved by two fitting parameters: the isotropic spin flip probabilities of the photogenerated electron and hole during their thermalization. We show that under the conditions of our quasi-resonant excitation, photogenerated electrons partially preserve their initial spin orientations, while holes completely dephase.

Acknowledgments

The support of the US-Israel binational science foundation (BSF), the Israeli science foundation (ISF), the ministry of science and technology (MOST) and that of the Technion's RBNI are gratefully acknowledged.

References

[1] D. Heiss, M. Kroutvar, J. J. Finley, and G. Abstreiter, Solid State Commun. **135**, 591 (2005).
[2] D. Loss and D. P. DiVincenzo, Phys. Rev. A. **57**, 120 (1998).
[3] D. Gershoni, Nature Materials **5**, 255, (2006).
[4] A. Imamoglu, D. D. Awschalom, G. Burkard, D. P. DiVincenzo, D. Loss, M. Sherwin, and A. Small, Phys. Rev. Lett. **83**, 4204, (1999).
[5] C. H. Bennet and G. Brassard, in *IEEE International Conference on Computers, Systems and Signal Processing* (IEEE, New York, 1984).
[6] F. Meier and B. P. Zakharchenya, Eds., *Optical Orientation* (North-Holland, Amsterdam, 1984).
[7] A. Ebbens, D. N. Krizhanovskii, A. I. Tartakovskii, F. Pulizzi, T. Wright, A. V. Savelyev, M. S. Skolnick, and M. Hopkinson, Phys. Rev. B. **72**, 073307 (2005).
[8] M. Atatüre, J. Dreiser, A. Badolato, A. Högele, K. Karrai, and A. Imamoglu, Science **312**, 551 (2006).
[9] X. Xu, Y. Wu, B. Sun, Q. Huang, J. Cheng, D. G. Steel, A. S. Bracker, D. Gammon, C. Emary, and L. J. Sham, Phys. Rev. Lett. **99**, 097401 (2007).
[10] B. D. Gerardot, D. Brunner, P. A. Dalgarno, P. Öhberg, S. Seidl, M. Kroner, K. Karrai, N. G. Stoltz, P. M. Petroff, and R. J. Warburton, Nature **451**, 441 (2008).
[11] A. J. Ramsay,1 S. J. Boyle, R. S. Kolodka, J. B. B. Oliveira, J. Skiba-Szymanska, H. Y. Liu, M. Hopkinson, A. M. Fox, and M. S. Skolnick, Phys. Rev. Lett. **100**, 197401 (2008).
[12] D. Press, T. D. Ladd, B. Zhang, and Y. Yamamoto, Nature **456**, 218 (2008).
[13] E. Dekel, D. Gershoni, E. Ehrenfreund, D. Spektor, J. M. Garcia, and P. M. Petroff, Phys. Rev. Lett. **80**, 4991 (1998).
[14] D. V. Regelman, U. Mizrahi, D. Gershoni, E. Ehrenfreund, W. V. Schoenfeld, and P. M. Petroff, Phys. Rev. Lett. **87**, 257401 (2001).
[15] D. Gammon, E. S. Snow, B. V. Shanabrook, D. S. Katzer, and D. Park, Phys. Rev. Lett. **76**, 3005 (1996).
[16] M. E. Ware, E. A. Stinaff, D. Gammon, M. F. Doty, A. S. Bracker, D. Gershoni, V. L. Korenev, Ş. C. Bădescu, Y. Lyanda-Geller, and T. L. Reinecke, Phys. Rev. Lett. **95**, 177403 (2005).
[17] N. Akopian, N. H. Lindner, E. Poem, Y. Berlatzky, J. Avron, D. Gershoni, B. D. Gerardot, and P. M. Petroff, Phys. Rev. Lett. **96**, 130501 (2006).
[18] M. Ediger, G. Bester, B. D. Gerardot, A. Badolato, P. M. Petroff, K. Karrai, A. Zunger, and R. J. Warburton, Phys. Rev. Lett. **98**, 036808 (2007).
[19] E. Poem J. Shemesh, I. Marderfeld, D. Galushko, N. Akopian, D. Gershoni, B. D. Gerardot, A. Badolato, and P. M. Petroff, Phys. Rev. B **76**, 235304 (2007).
[20] M. Paillard, X. Marie, P. Renucci, T. Amand, A. Jbeli, and J-M. Gérard, Phys. Rev. Lett. **86**, 1634 (2001).
[21] R. J. Young, S. J. Dewhurst , R. M. Stevenson, P. Atkinson, A. J. Bennett, M. B. Ward, K. Cooper, D. A. Ritchie, and A. J. Shields, New J. Phys. **9**, 365 (2007).
[22] I. Favero, G. Cassabois, C. Voisin, C. Delalande, Ph. Roussignol, R. Ferreira, C. Couteau, J. P. Poizat, and J-M. Gérard, Phys. Rev. B. **71**, 233304 (2005).
[23] A. S. Bracker, E. A. Stinaff, D. Gammon, M. E. Ware, J. G. Tischler, A. Shabaev, Al. L. Efros, D. Park, D. Gershoni, V. L. Korenev, and I. A. Merkulov, Phys. Rev. Lett. **94**, 047402 (2005).
[24] P. Borri, W. Langbein, S. Schneider, U. Woggon, R. L. Sellin, D. Ouyang, and D. Bimberg, Phys. Rev. Lett. **87**, 157401 (2001).
[25] A. I. Tartakovskii, J. Cahill, M. N. Makhonin, D. M. Whittaker, J-P. R. Wells, A. M. Fox, D. J. Mowbray, M. S. Skolnick, K. M. Groom, M. J. Steer, and M. Hopkinson, Phys. Rev. Lett. **93**, 057401 (2004).
[26] P-F. Braun, B. Eble, L. Lombez, B. Urbaszek, X. Marie, T. Amand, P. Renucci, O. Krebs, A. Lemaître, P. Voisin, V. K. Kalevich, and K. V. Kavokin, Phys. Stat. Sol. (b) **243**, 3917 (2006).
[27] S. Laurent, M. Senes, O. Krebs, V. K. Kalevich, B. Urbaszek, X. Marie, T. Amand, and P. Voisin, Phys. Rev. B. **73**, 235302 (2006).
[28] S. Cortez, O. Krebs, S. Laurent, M. Senes, X. Marie, P. Voisin, R. Ferreira, G. Bastard, J-M. Gérard, and T. Amand, Phys. Rev. Lett. **89**, 207401 (2002).
[29] V. K. Kalevich, I. A. Merkulov, A. Yu. Shiryaev, K. V. Kavokin, M. Ikezawa, T. Okuno, P. N. Brunkov, A. E. Zhukov, V. M. Ustinov and Y. Masumoto, Phys. Rev. B **72**, 045325 (2005).
[30] A. Shabaev, E. A. Stinaff, A. S. Bracker, D. Gammon, Al. L. Efros V. L. Korenev, and I. Merkulov, Phys. Rev. B. **79**, 035322 (2009).
[31] D. Heiss, S. Schaeck, H. Huebl, M. Bichler, G. Abstreiter, J. J. Finley, D. V. Bulaev, and D. Loss, Phys. Rev. B. **76**, 241306(R) (2007).
[32] V. N. Golovach, A. Khaetskii, and D. Loss, Phys. Rev. Lett. **93**, 016601 (2004).
[33] E. Dekel, D.V. Regelman, D. Gershoni, E. Ehrenfreund, W.V. Schoenfeld, and P.M. Petroff, Solid State Commun. **117**, 395 (2001).
[34] R. I. Dzhioev, B. P. Zakharchenya, E. L. Ivchenko, V. L. Korenev, Yu. G. Kusraev, N. N. Ledentsov, V. M. Ustinov, A. E. Zhukov, and A. F. Tsatsulnikov, Pis'ma Zh. Eksp. Teor. Fiz. **65**, 766 (1997).